

## Calibration Free Laser Induced Breakdown Spectroscopy (CF-LIBS) as a tool for Quantitative Elemental Analysis of Iraqi Cement

Tagreed K. Hamad<sup>1</sup>, Alaa H. Ali<sup>2</sup>, Hussein T. Salloom<sup>3</sup> and Alaa J. Ghazai<sup>1</sup>

<sup>1</sup> Physics Dept. Science College, Al-Nahrain University, Iraq.

<sup>2</sup> Material research Dept. Ministry of Science and Technology, Iraq.

<sup>3</sup> Al-Nahrain Nanorenewable Energy Center, Al-Nahrain University, Iraq.

### Abstract

Laser-induced breakdown spectroscopy (LIBS) is a promising atomic emission based elemental analysis technique that has many potential applications for various samples. This paper presents the implementation of calibration free laser induced breakdown spectroscopy (CF-LIBS) approach to identify and determine the concentration of elements in Iraqi cement samples collected from local market. Q-switched Nd: YAG laser with energy laser pulse of 100 mJ and pulse duration of 9 ns is focused on cement pellet surface to generate a plasma spark in air. The plasma emission spectrum was recorded by the spectrometer connected to the fiber optic and resolved spectra were used for identification and quantification of detected elements. The produced plasma temperature was obtained from the Boltzmann plot method while their electron density was determined by Saha-Boltzmann equation. The major elements such as Ca, Si, Al, Fe, Mg and minor Mn, Ti, K and Na elements have been identified and their concentrations calculated based on analysis of the spectrum that contain all information needed to derive the elemental composition of the cement matrix.

[DOI: [10.22401/ANJS.00.1.08](https://doi.org/10.22401/ANJS.00.1.08)]

**Keywords:** Calibration-Free LIBS, Quantitative analysis, Iraqi Cement, Spectral analysis.

### Introduction

Recently, Laser-induced breakdown spectroscopy (LIBS) has shown a great potential as an effective analytical tool for detection of elements with several advantages over conventional techniques [1], [2]. It is a fast, in situ and reliable multi elemental analysis of any states of materials that consuming only some micrograms of the samples [3], [4]. Considering the solid materials, LIBS analysis has been applied not only for the simple metals matrix but also for complex matrix such as soil, rocks and cultural heritage objects [5]-[7]. In brief, LIBS is a type of atomic emission spectroscopy where pulsed laser with high enough power density strikes the surface of the sample to generate a plasma at that surface, then the emission of characteristics lines for elements presented in the sample will occur to give a unique fingerprint [3]. Quantitative LIBS analysis can be performed either based on construction of calibration curves using standard matched matrix, or based on calibration free where no need for calibration curves. As proposed by *Ciucci et al* [8], the CF-LIBS analysis can be applied to any element in the periodic table provided that a relevant spectral information

must be obtained. It is based on analyzing the physics of the plasma process and experimentally validate local thermal equilibrium and thin plasma conditions[9]. CF-LIBS technique has been successfully employed for metallic alloys and oxides, *Pandhija et al.* determined the concentration of toxic heavy metals in soil of industrial area [10]. *Praher et al.* presented quantitative determination of element concentrations in industrial oxide materials by CF-LIBS [11].

Cement is a fine powder, obtained from the firing at 1,400 °C of a mix of limestone, clay, and iron ore. The firing process produced the main ingredient of cement called clinker, which is finely ground with gypsum and other chemical additives to produce cement. To validate a good control of quality and operation in best condition, the understanding of the chemical compositions of raw materials and product are essential. Nowadays, elemental composition analysis of cement is performed by AAS and XRF in cement factories, Although XRF are widely used for characterizing cement, it has many drawbacks such as need for sample preparation, expensive apparatus and poor sensitivity to detect light elements [12]. Therefore, further investigation

is necessary to explore alternative analytical tool. In the present work, the assessment of using CF-LIBS for quantitative analysis of major, minor and the trace elements presented in Iraqi cement samples collected from Mass factory has been investigated. The obtained results have also compared with those obtained from XRF analysis.

## 2. Experimental Procedure

### 2.1. LIBS system

The experimental set up used for LIBS analysis of cement samples is shown in Fig.(1). Samples were irradiated by nanosecond Q-switched Nd: YAG laser operating at wavelength of 1064 nm, pulse width of 9 ns, output pulse energy was 100 mJ. The laser beam is focused by a convex lens with focal length of 100 mm on the sample surface. The diameter of the focused laser spot is 0.028 mm and the peak power is in the order of  $11.1 \times 10^6$  W.

The emission of plasma was collected by a imaging lens with diameter of 15 mm, and focused onto optical fiber type (SMA, 50  $\mu$ m/0.22 NAc, which deliver the plasma light to the entrance slit of spectrum analyzer model (CCS-100) with (1200 Line/ mm) grating and slit dimension of 20  $\mu$ m. The grating disperses light according to wavelength and then reflected by mirrors to detect and convert optical signals to digital, and then moves the digital signal to the application. Each emission spectrum obtained by integration of 10 laser shots impinging on surface of the sample. Specific software was utilized to illustrate the data as a diagram between intensity and wavelength. The experiment is performed under fixed environment conditions.

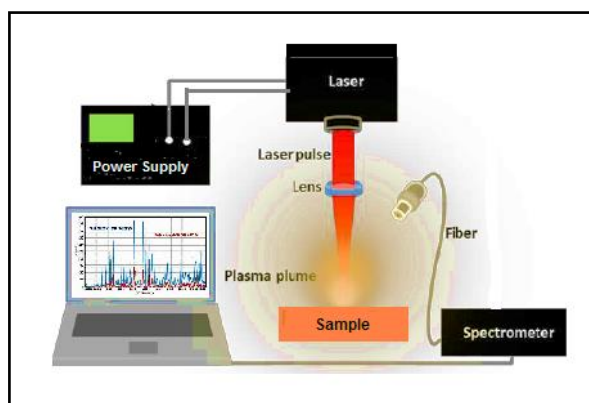


**Fig.(1) Experimental set up for LIBS Measurements.**

### 2.2. Preparation of experimental samples

There are several brands of cement available at Iraqi market; their chemical compositions are the same. Variations in physical properties occur due to the variation of constituents. In this study, two different types of cement produced at Mass factory were used. Firstly, Ordinary Portland cement (OPC) was used in general construction. Secondly, Sulfate resistance cement (SRC) was used especially for foundations in civil construction. A pressed pellet is prepared from 3.0 gram of each cement. Hydraulic pressure machine model (Auto Series) was used to press the powder cement without binder at (7.0 ton) to a disc of 1.0 cm diameter and 5.0 mm thick. To conduct elemental composition of cement samples, X-ray fluorescence model multi channel MXF2400 from Shimadzu was used. In cement analysis, Ca, Si, Al, Fe, Mg, Mn, Ti, K and Na are expressed as the CaO, SiO<sub>2</sub>, Al<sub>2</sub>O<sub>3</sub>, Fe<sub>2</sub>O<sub>3</sub>, MgO, Mn<sub>2</sub>O<sub>3</sub>, TiO<sub>2</sub>, K<sub>2</sub>O and Na<sub>2</sub>O oxides form. These oxides eventually become more complex compounds responsible for main cement properties such as early strength, set times and color effects [13]. The obtained XRF results are finally compared with related CF-LIBS data.

## 3. Results and discussion

### 3.1 Calibration free assumptions

The detailed description of CF LIBS can be found in [9], it based on the assumption of local thermal equilibrium, stoichiometric ablation and optically thin plasma. These assumptions need to be validated before performing CF- LIBS Quantitative analysis.

Stoichiometric ablation ensures plasma plume and then the emission spectrum have the same composition as the considered material, laser ablation of cement was achieved by a Q- Switched Nd: YAG laser of 1064 nm with 9 ns pulse duration and a focal spot diameter of 0.028 mm. The power density is calculated to be  $5.66 \times 10^{12}$  W/cm<sup>2</sup> which is enough to induced ionization and generate plasma on the sample surface and satisfies the condition of stoichiometric ablation.

Optically thin plasma condition is necessary to ensure that other atoms in a lower energy state do not reabsorb the radiation emitted by an excited atom and avoid the so-called self-absorption effect. In the absence of

self-absorption, the intensity ratio of two emission lines from the same species, having the same upper energy level should be similar to the ratio of their corresponding transition probabilities. The experimentally observed intensity ratio of various spectral lines of Ca I, Fe I and Si II have been used and compared them with the ratio of their transition probabilities. Table (1) presents the intensity ratio and transition probability ratio between two Ca lines of 443.569 nm and 442.544 nm,

Fe lines of 647.562 nm and 657.501 nm, Si of 634.718 and 385.602 nm. The intensity ratio for Ca I/ Ca I was 0.68 and their transition ratio was similar. The intensity ratio for Fe I/ Fe I was 0.6 and their transition ratio was 0.604. The consistency between the intensities of Ca, Fe, Si and with their corresponding transition probability was observed, which clearly supported the assumption of optically thin laser induced plasma [14].

**Table (1)**  
**Comparison between the intensity ratio of two non-resonant lines of Ca I, Fe I and Si II and the ratio of their corresponding transition probabilities.**

Element	Wavelength (nm)	Upper Energy Level (eV)	Transition probability	Intensity ratio	Transition probability ratio
Ca I	443.569	4.680179	1.03*10 <sup>8</sup>	0.68	0.69
	442.544	4.680179	1.49*10 <sup>8</sup>		
Fe I	647.562	4.47327	1.82*10 <sup>5</sup>	0.60	0.604
	657.501	4.47327	3.01*10 <sup>5</sup>		
Si II	385.602	10.073	1.76*10 <sup>8</sup>	0.727	0.724
	634.710	10.073	2.34*10 <sup>8</sup>		

In local thermal equilibrium condition, the collision process predominate the radiative process, which ensures that the energy exchange between the species is larger than the energy lose due to the radiation. The basic criterion used for LTE validation is Mc Whirter criterion, which defines the lower limit of electron density to ensure enough collisions for the existence of LTE and is given by:

$$N_e(cm^{-3}) \geq 1.6 * 10^{12} * \sqrt{T} * (\Delta E)^3 \dots\dots (1)$$

where  $\Delta E$  (eV) is the highest energy transition.

The electron density is estimated from stark broadening of spectral line. For the linear Stark effect, the electron density  $N_e$  and the full width at half maximum  $\Delta\lambda_{FWHM}$  of spectral line are related by the following relation [15]:

$$N_e = 2W \left( \frac{\Delta\lambda_{FWHM}}{10^{16}} \right) \dots\dots\dots (2)$$

$W$  is a constant called the electron impact parameter.

Fig.(2) shows the experimental observed data points of Ca II emission line as (●) and the full red line, which approximately passes through all the points is the Lorentz distribution function fit. From this figure, the FWHM of the experimental emission of this line equal 0.43 nm. By substituting this value and using the value of impact parameter  $w = 0.286$  [16] in Eq. 2,  $N_e$  is calculated to be  $7.5 \times 10^{16} \text{ cm}^{-3}$ .

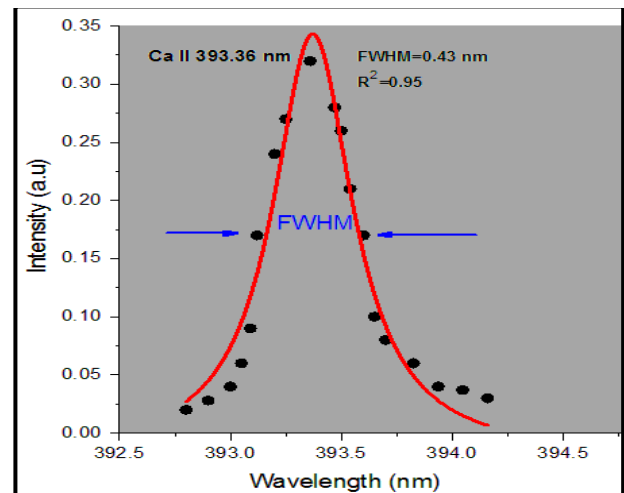


**Fig.(2) Stark broadening of Ca II spectral line 393.36 nm used to calculate the electron density  $N_e$  from plasma of ordinary Mass cement sample. Experimental data (black dot) fits a Lorentzian curve (red curve).**

Plasma temperature have been determined from the relative intensities of the emission lines of all presented elements using the Boltzmann plot method [17]. The observed emission spectra contain spectral lines of Ca I, Si I, Si II, Al I, Fe I, Mg I, Mn I, Mn II, Ti I, K I, Na I and Ba I, which have been used to construct the Boltzmann plot to extract the plasma temperature. The atomic parameters of selected lines were taken from NIST database [18] and are listed in Table (2).

**Table (2)**  
**Spectrometric parameter of the emission lines of cement sample.**

Element	wavelengths	A*g (s <sup>-1</sup> )	Ei (eV)	T(eV) Ordinary Mass	T(eV) Resistance Mass
Ca I	364.441	2.48E8	5.3000	0.829	0.83
	428.3	2.17E8	4.7790		
	487.81	1.32E8	5.2499		
	612.22	8.61E7	3.9100		
Si I	564.56	4.8E6	7.1250	0.833	0.84
	568.44	7.8E6	7.1340		
	672.18	1.7E7	7.7060		
	700.35	2.39E7	7.7530		
Si II	412.507	8.94E8	12.839	0.820	0.82
	505.59	8.7E8	12.525		
	595.75	1.12E8	12.140		
	634.71	2.34E7	10.073		
Al I	555.79	9.2E5	5.3728	0.823	0.826
	555.706	9.2E5	5.3734		
	669.86	2.0E6	4.9930		
	736.15	1.39E7	5.7057		
Al II	390.06	2.4E6	10.598	0.832	0.833
	466.3	1.74E8	13.250		
	559.33	4.63E8	15.470		
	704.21	2.89E8	13.076		
Fe I	379.85	3.55E7	4.1770	0.826	0.82
	387.85	1.85E7	3.2800		
	432.57	3.61E8	4.4700		
	495.75	4.64E8	5.3080		
Mg I	405.75	5.1E7	7.4006	0.833	0.830
	416.72	6.9E7	7.3200		
	435.19	9.2E7	7.1939		
	470.29	1.1E8	6.9810		
	552.84	6.95E7	6.5870		
Mn I	357.78	7.5E8	5.5785	0.835	0.84
	401.8	2.03E8	5.1989		
	403.9	3.8E7	6.8320		
	404.13	3.0E8	5.2251		
	408.29	1.7E8	5.2139		
	475.4	2.42E8	4.8880		
Mn II	420.63	1.08E7	8.3430	0.83	0.82
	429.22	1.0E7	8.2681		
	434.39	2.8E7	8.2502		
	721.99	7.5E8	12.380		
Ti I	388.2	2.24E9	5.2327	0.816	0.822
	399.86	4.33E8	3.1477		
	451.27	1.08E8	3.5800		
	466.75	2.26E7	2.6760		
	499.95	4.74E8	3.3050		
	503.99	2.2E7	2.4800		
	521.03	3.5E7	2.4260		
K I	496.50	1.6E6	4.1135	0.844	0.823
	508.422	7.0E5	4.0973		
	511.224	2.1E6	4.0416		
	5.33.96	2.52E6	3.9344		
Na I	417.2	2.8E8	36.240	0.844	0.826
	418.55	2.9E8	36.250		
	443.23	8.4E7	35.496		
	507.12	2.5E8	35.560		
Ba I	350.11	1.05E8	3.5403	0.826	0.83
	577.54	5.6E8	3.8200		
	582.62	1.35E8	3.5402		
	634.16	8.4E7	3.0970		

The Boltzmann plot of cement sample are presented in Fig.(3), plasma temperatures of ordinary and resistance Mass cements have been calculated from the slopes of the straight lines as listed in Table (2). For the calibration free analysis, an average value of the plasma temperature 0.83 K and 0.827 K have been used respectively.

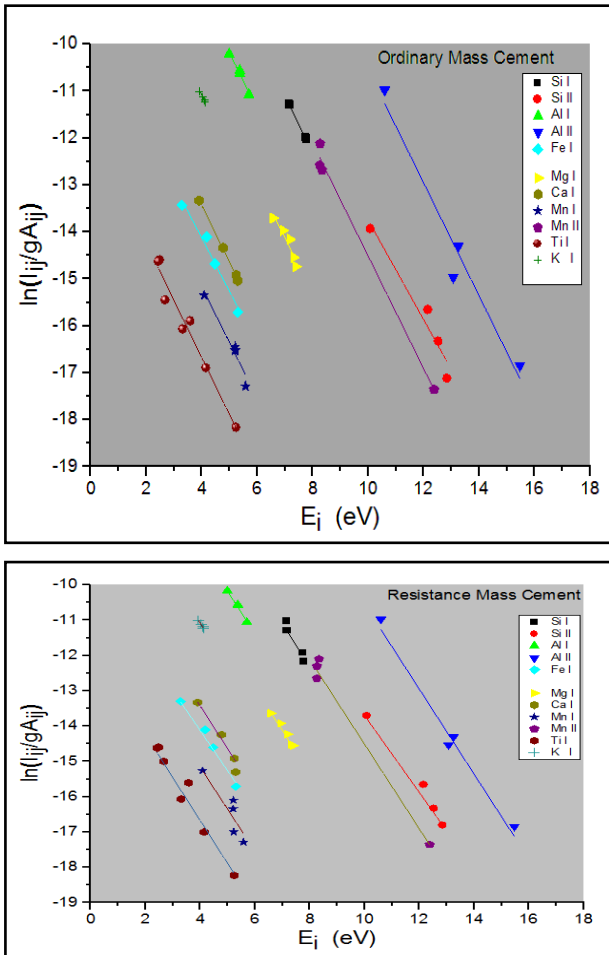


**Fig.(3): Family of lines in Boltzmann Plot derived from LIBS of Si I, Si II, Al I, Al II, Fe I, Mg I, Ca I, Mn I, Mn II, Ti I, K I species of ordinary and resistance Mass Cement samples.**

The condition of local thermodynamic equilibrium (LTE) was checked for obtained electron density and plasma temperature for the Ca I line at 443.569 nm. By substituting  $\Delta E = 3.12 \text{ eV}$  and plasma temperature  $T_e = 0.83 \text{ eV}$ , the limit of electron density is calculated using Eq. 1 to be  $14.18 \times 10^{12} \text{ cm}^{-3}$ , which is much lower than that experimentally determined from the Stark broadened spectral lines. Thus, the generated plasma is within LTE.

The electron density was also determined by employing Saha-Boltzmann that relates the number density of a particular element in the two consecutive charged states  $N^{II}$ ,  $N^I$  as following [19]:

$$N_e = 6.04 * 10^{24} (T)^{3/2} \left(\frac{I\lambda}{gA}\right)_{ion} \left(\frac{gA}{I\lambda}\right)_{atom} \times \exp\left[-\frac{(V^+ + E_{ion} - E_{atom})}{K_B T}\right] \dots\dots\dots(3)$$

By using the intensity of the neutral and singly ionized spectral lines and the spectroscopic parameters and ionization energies enlisted in Table (3) of all elements for both ordinary Portland and sulfite resistance Mass cement, the values of  $N_e$  for each element have been determined and will be used for the subsequent CF LIBS calculations.

**Table (3)**  
**Spectroscopic parameters and the ionization energies of all elements presented in Cement samples.**

Element	Ei	Ea	Wi	Wa	<i>N<sub>e</sub></i> ordinary Mass	<i>N<sub>e</sub></i> resistance Mass
Ca	10.45	2.325	420.61	422.67	5.60×10 <sup>12</sup>	6.44×10 <sup>12</sup>
Si	14.79	5.0823	546.68	390.55	5.25×10 <sup>10</sup>	4.55×10 <sup>10</sup>
Al	17.7	3.14	458.97	396.15	1.45×10 <sup>11</sup>	1.56×10 <sup>11</sup>
Fe	12.77	4.47	506.78	352.616	4.82×10 <sup>14</sup>	3.08×10 <sup>14</sup>
Mg	12.822	5.94	439.05	383.82	3.95×10 <sup>11</sup>	5.21×10 <sup>11</sup>
Mn	8.2502	5.18	434.39	404.14	3.18×10 <sup>15</sup>	4.95×10 <sup>15</sup>
Ti	3.9043	3.3365	375.92	498.17	3.05×10 <sup>15</sup>	3.17×10 <sup>15</sup>
K	23.355	4.222	381.75	474.43	5.7×10 <sup>13</sup>	7.00×10 <sup>13</sup>
Na	36.354	36.245	363.12	388.18	3.3×10 <sup>17</sup>	4.5×10 <sup>17</sup>
Ba	2.721	3.82	585.36	577.76	7.5×10 <sup>17</sup>	6.77×10 <sup>17</sup>

**3.2 Calculations of elemental composition**

From the above discussion, one can deduce that the generated plasma is in LTE and optically thin so that calibration free can be used for quantitative analysis of constituent elements in cement samples. The concentration of the species *C<sub>s</sub>* is evaluated from the intercepts of the fitted lines in the Boltzmann plot Fig.(3); each intercept is a function of the number density (*n<sub>s</sub>*) of the individual species (*s*) in the plasma. The species concentrations of any element in the plasma could be determined from the emission of one neutral line according to:

$$C^s = \frac{1}{F} U^s(T) e^{q^s} \dots\dots\dots (4)$$

where *U<sup>s</sup>(T)* is the partition function, *q<sup>s</sup>* is the intersection value of the linear regression in the Boltzmann plane. The concentration of a specific element of interest is given by the sum of the concentrations of neutral and singly ionized species [20]. When it is difficult to observed lines of ionized states and not possible to draw their Boltzmann plot, only the concentration *N<sup>I</sup>* of one species of a given element could be known. Then, the concentration *N<sup>II</sup>* of the other ionization states can be calculated using Saha-Boltzmann equation, which can be written as:

$$\frac{N_e N^{II}}{N^I} = \frac{2U^{II}(T)}{U^I(T)} \frac{2\pi m_e k_B}{h^3} e^{-\frac{E_{ion}}{k_B T}} \dots\dots\dots (5)$$

where *N* is the number density for neutral atoms *I* and singly ionized atoms *II*.

CF-LIBS approach requires an extensive calculation for which an Origin program has been used to calculate the concentrations. The inputs were the values of the slope, intercepts and the list of transition probabilities and degeneracy belong to each element. The concentration of all different elements presented in ordinary and resistance Mass cement using CF LIBS are summarized in Table (4).

**Table (4)**  
**Concentration of Ca, Si, Al, Fe Mg, Mn, Ti, K, Na, and Ba in Two different samples (ordinary and resistance Mass cement) estimated by CF-LIBS.**

Element detected	Atomic weight	E <sub>ion</sub>	U <sub>z</sub>	U <sub>z+1</sub>	Ordinary Mass %	Resistance Mass %
Ca	40.07	6.11	4.91	5.85	45.8	45.34
Si	28.08	8.15	11.16	5.85	10.22	10.02
Al	26.98	5.985	6.83	1.03	2.83	2.04
Fe	55.8	7.902	56.04	64.85	2.15	2.95
Mg	24.3	7.64	1.53	2.03	1.227	1.10
Mn	54.93	7.43	14.07	13.72	0.127	0.24
Ti	47.86	6.82	77.35	81.62	0.19	0.17
K	39.09	4.34	8.64	1	0.33	0.32
Na	22.98	5.13	15.6	1	0.214	0.09
Ba	137.3	5.21	14.71	6.79	0.084	0.071

Within this CF LIBS, analysis of spectra confirmed presence of major and minor elements. In addition, this method is utilized to detect trace element such as barium Ba with quantitative information about it. These quantitative elemental analysis are compared with the results obtained from XRF, the

absolute and relative errors are also calculated and listed in Table. (5). The highest value of relative error percentage was 5% for titanium while the lowest value was 0.24 for magnesium. These error could be attributed to uncertainties associated mainly with the determination of plasma temperature.

**Table (5)**  
**Absolute error (A.E), Relative error (R.E) of elements composition of ordinary Mass cement calculated by CF-LIBS and XRF methods.**

Elements	XRF	CF-LIBS	A.E	R.E %
Ca	45.2	45.8	0.6	1.3
Si	10.55	10.22	0.33	3.12
Al	2.83	2.83	0.01	0.354
Fe	2.14	2.15	0.01	0.46
Mg	1.23	1.227	0.003	0.243
Mn	0.124	0.127	0.003	2.41
Ti	0.2	0.19	0.01	5
K	0.34	0.33	0.01	2.94
Na	0.21	0.214	0.004	1.904

In general, two techniques have comparable results for elements concentrations analysis, Fig. (4) shows the bar diagram of the data of Si, Al, Fe, Mg, Mn, Ti, K and Na that listed in Table (6). The same trends in the relative changes of element concentration are noticed in two techniques; however, the analytical results are not completely correspond for each other. Each technique has significant procedure and regulation to detect

the elements of cement, which make these techniques with advantage and disadvantage. Among these technique the interaction between the laser and the sample in LIBS is influenced significantly by the overall sample composition, so that the intensity of the emission lines observed is a function of both the concentration of the elements and the matrix properties that contain them [21], [22].

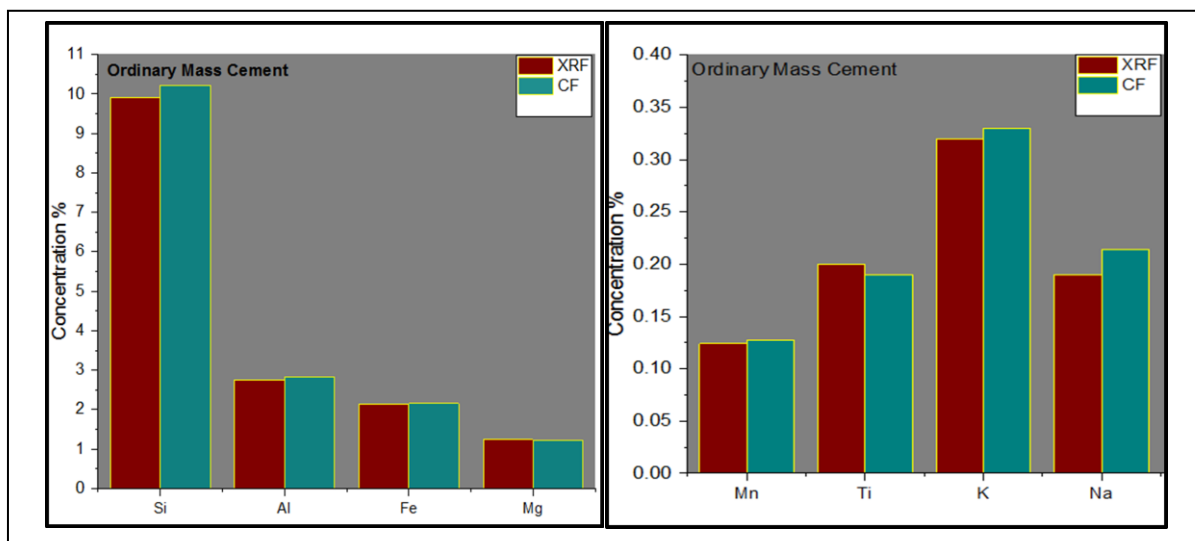


**Fig.(4) Element concentration of Si, Al, Fe, Mg, Mn, Ti, K and Na in ordinary Mass cement calculated with LIBS and other analysis techniques.**

Besides the major and minor elements which including in cement and give acceptable information, the detection of trace elements is required as shown in Fig.(5) the ability to detect these element is significant and give power to instrument have been used, since in XRF technique the basic principle of operation is the detection of x-ray fluorescence, so it could not analyze the light elements with atomic number less than 11 such as Ba which present a problem [23].

### Conclusions

A calibration-free LIBS algorithm was implemented and tested by mathematical analyzing of LIBS spectra for quantitative analysis of Iraqi cement samples. The plasma temperature and electron number density were determined from Saha-Boltzmann plots and the calcium line width respectively. The LIBS spectra of pressed cement samples have been measured and employed for composition analysis using CF-LIBS approach. The calculated metals concentration was close to the XRF analysis results, the highest value of relative error percentage was 5% for titanium while the lowest value was 0.24 for magnesium. Our results shows that the calibration-free LIBS method is a promising approach for the quantitative determination of major and minor element and oxide concentration. Various applications of CF-LIBS can be proposed including on-site and in-line analysis in industrial and biological materials.

### References

- [1] M. E. Sigman, D. Ph, E. M. Mcintee, and C. Bridge, "Application of Laser-Induced Breakdown Spectroscopy to Forensic Science: Analysis of Paint Samples", 2012.
- [2] L. Edwards, "Laser-induced breakdown spectroscopy for the determination of carbon in soil", UNIVERSITY OF FLORIDA, 2007.
- [3] David A. Cremers et al, *Handbook of Laser-Induced Breakdown Spectroscopy Second Edition*. 2013.
- [4] A. M. Ollila, "Analyzing Geological Materials Under Martian Conditions Using Laser-Induced Breakdown Spectroscopy: Plasma Fundamentals, Sample Classification, and Trace Element Quantification", *Earth Environ. Sci.*, 2003.
- [5] M. A. Khater, "Trace detection of light elements by laser-induced breakdown spectroscopy (LIBS): Applications to non-conducting materials", *Opt. Spectrosc.*, vol. 115, no. 4, pp. 574-590, 2013.
- [6] A. Erdem *et al.*, "Characterization of Iron age pottery from eastern Turkey by laser-induced breakdown spectroscopy (LIBS)", *J. Archaeol. Sci.*, vol. 35, no. 9, pp. 2486-2494, 2008.
- [7] R. S. Harmon *et al.*, "Laser-induced breakdown spectroscopy-An emerging chemical sensor technology for real-time field-portable, geochemical, mineralogical, and environmental applications", *Appl. Geochemistry*, vol. 21, no. 5, pp. 730-747, 2006.

- [8] G. S. Senesi *et al.*, “Heavy metal concentrations in soils as determined by laser-induced breakdown spectroscopy (LIBS), with special emphasis on chromium”, *Environ. Res.*, vol. 109, no. 4, pp. 413-420, 2009.
- [9] E. Tognoni, G. Cristoforetti, S. Legnaioli, and V. Palleschi, “Calibration-Free Laser-Induced Breakdown Spectroscopy: State of the art”, *Spectrochim. Acta-Part B At. Spectrosc.*, vol. 65, no. 1, pp. 1-14, 2010.
- [10] S. Pandhija, N. K. Rai, A. K. Rai, and S. N. Thakur, “Contaminant concentration in environmental samples using LIBS and CF-LIBS”, *Appl. Phys. B Lasers Opt.*, vol. 98, no. 1, pp. 231-241, 2010.
- [11] B. Praher, V. Palleschi, R. Viskup, J. Heitz, and J. D. Pedarnig, “Calibration free laser-induced breakdown spectroscopy of oxide materials”, *Spectrochim. Acta - Part B At. Spectrosc.*, vol. 65, no. 8, pp. 671-679, 2010.
- [12] A. Mansoori, B. Roshanzadeh, M. Khalaji, and S. H. Tavassoli, “Quantitative analysis of cement powder by laser induced breakdown spectroscopy”, *Opt. Lasers Eng.*, vol. 49, no. 3, pp. 318-323, 2011.
- [13] B. R. J. Muhyedeen and L. K. Mizhir, “Analysis of Iraqi cement by X-ray Fluorescence”, *Iraqi J. Chem.*, vol. 27, no. 4, pp. 1-14, 2001.
- [14] M. Achouri, T. Baba-Hamed, S. A. Beldjilali, and A. Belasri, “Determination of a brass alloy concentration composition using calibration-free laser-induced breakdown spectroscopy”, *Plasma Phys. Reports*, vol. 41, no. 9, pp. 758-768, 2015.
- [15] C. Aragón and J. A. Aguilera, “Characterization of laser induced plasmas by optical emission spectroscopy: A review of experiments and methods”, *Spectrochim. Acta - Part B At. Spectrosc.*, vol. 63, no. 9, pp. 893-916, 2008.
- [16] J. R. F. and W. L. W. N. Konjevic, Lesage, A, “Experimental Stark Widths and Shifts for Spectral Lines of Neutral and Ionized Atoms”, *J. Phys. Chem. Ref. Data*, vol. 31, no. 3, 2002.
- [17] I. Borgia *et al.*, “Self-calibrated quantitative elemental analysis by laser-induced plasma spectroscopy: application to pigment analysis”, *J. Cult. Herit.*, vol. 1, pp. S281-S286, 2000.
- [18] A. Kramida, Y. Ralchenko, J. Reader, and NIST ASD Team, “NIST Atomic Spectra Database Lines Form”, *NIST Atomic Spectra Database (ver. 5.2) [Online]*, 2014. [Online]. Available: <http://physics.nist.gov/asd>.
- [19] N. Ahmed, R. Ahmed, M. Rafiqe, and M. A. Baig, “A comparative study of Cu–Ni Alloy using LIBS, LA-TOF, EDX, and XRF”, *Laser Part. Beams*, pp. 1-9, 2016.
- [20] T. Takahashi, B. Thornton, K. Ohki, and T. Sakka, “Calibration-free analysis of immersed brass alloys using long-nanosecond pulse laser-induced breakdown spectroscopy with and without correction for nonstoichiometric ablation”, *Spectrochim. Acta-Part B At. Spectrosc.*, vol. 111, pp. 8-14, 2015.
- [21] D. M. Díaz Pace, N. a. Gabriele, M. Garcimuño, C. a. D’Angelo, G. Bertuccelli, and D. Bertuccelli, “Analysis of Minerals and Rocks by Laser-Induced Breakdown Spectroscopy”, *Spectrosc. Lett.*, vol. 44, no. 6, pp. 399-411, 2011.
- [22] W. LUO, X. ZHAO, S. LV, and H. ZHU, “Measurements of egg shell plasma parameters using laser-induced breakdown spectroscopy”, *Pramana*, vol. 85, no. 1, pp. 105-114, 2015.
- [23] N. Taefi, M. Khalaji, and S. H. Tavassoli, “Determination of elemental composition of cement powder by Spark Induced Breakdown Spectroscopy”, *Cem. Concr. Res.*, vol. 40, no. 7, pp. 1114-1119, 2010.